

Topological susceptibility and QCD phase transition with 2+1 flavor Möbius domain wall fermion at finite temperature

Issaku Kanamori,^{a,*} Yasumichi Aoki,^a Hidenori Fukaya,^b Jishnu Goswami,^c Shoji Hashimoto^{d,e} and Yu Zhang^c (JLQCD collaboration)

^aRIKEN Center for Computational Science (R-CCS), Kobe 650-0047, Japan

^bDepartment of Physics, Osaka University, Toyonaka, Osaka 560-0043, Japan

^cFakultät für Physik, Universität Bielefeld, Bielefeld, 33615, Germany

^dKEK Theory Center, High Energy Accelerator Research Organization (KEK), Tsukuba 305-0801, Japan

^eSchool of High Energy Accelerator Science, Graduate University for Advanced Studies (SOKENDAI), Tsukuba 305-0801, Japan

E-mail: kanamori-i@riken.jp, yasumichi.aoki@riken.jp,
hfukaya@het.phys.sci.osaka-u.ac.jp, jishnu@physik.uni-bielefeld.de,
shoji.hashimoto@kek.jp, yzhang@physik.uni-bielefeld.de

The topological susceptibility is one of the quantities that has a large discretization error, and the error can be sensitive to the choice of fermion action. We report on our results from physical point simulations with 2+1 flavor Möbius domain wall fermion at finite temperature. We also present the chiral condensate and disconnected susceptibility. The temporal lattice size is $N_t = 12$ and 16, and the temperature range is around 140 MeV to 250 MeV for the chiral condensate and susceptibility. A coarse lattice with $N_t = 10$ covers up to 500 MeV to measure the topological susceptibility.

*The 42nd International Symposium on Lattice Field Theory (LATTICE2025)
2-8 November 2025
Tata Institute of Fundamental Research, Mumbai, India*

*Speaker

1. Introduction

The chiral symmetry is the most important symmetry in QCD. It is therefore desirable to keep the chiral symmetry as much as possible in the lattice simulation. Möbius domain wall fermion (MDWF) is an optimal choice of the lattice fermion that keeps a balance between the chiral symmetry and the computational cost. In this talk, we use 2+1 flavor MDWF fermion at the physical point at finite temperature and present our preliminary results of chiral condensate/susceptibility and topological susceptibility.

Topological susceptibility is one of the fundamental quantities that characterizes the vacuum of QCD. The behavior at high temperature also plays an important role in the axion dark matter scenario. However, it is known that it may have a large discretization error depending on the discretizations of fermions. We need to quantify the discretization effects as well as possible systematic errors, which is especially challenging at high temperature. Because of the topology freezing at high temperature, sampling over topological sectors becomes difficult. We also need to use a very fine lattice to resolve the temporal direction. The results reported so far [1–7] in fact show a large discrepancy among the collaborations. Even among the results with the domain wall fermion, TWQCD reported a significantly larger value at high temperature than other collaborations with their optimal domain wall simulation [4]. As reported by Gavai et al. [7], Möbius domain wall fermion has small discretization errors, of which the detailed simulation setting is different from ours. They showed that $N_t = 8$ lattice result is already very close to the continuum limit with HISQ fermion. A new result with overlap fermion [8, 9] with $N_t = 8$ has appeared recently.

We also present the chiral condensate and disconnected susceptibility¹. They are, of course, important quantities to investigate the restoration of chiral symmetry at high temperature. Keeping a good chiral symmetry with MDWF helps to control systematic errors caused by the lattice artifact that breaks the chiral symmetry. With finite fifth-dimensional extent, the quark mass receives an additive contribution known as the residual mass, which contributes to the additive divergence that must be removed during renormalization. The result we present in this contribution implies that we have good control of the residual mass correction. Furthermore, the crossover transition temperature at the physical point read off from the peak location of the chiral susceptibility is consistent with results obtained from the HISQ and stout actions in the continuum limit [10, 11].

After explaining the simulation setting in the next section, we first present the result on chiral condensate and disconnected susceptibility in Sec. 3. Then, we show the behavior of topological charge and susceptibility in Sec. 4. Section 5 is for the summary and outlook.

2. Simulation Setup

We use Möbius domain-wall fermion with the scale factor 2 and gauge action with tree-level Symanzik-improvement. For the gauge field inside the fermion action, we apply 3 steps of stout smearing with the smearing parameter $\rho = 0.1$. The details of the action used in the JLQCD collaboration are found in the supplement material of [12].

¹We originally planned to deliver the results of these quantities by Y.Z. as an independent talk, but had not realized because she could not attend the conference on site.

The quark masses are set to the physical point along the line of constant physics, where the renormalized light quark mass m_l^R is set to $1/27.4$ of the strange quark mass m_s^R at the renormalization scale $\mu = 2$ GeV. The dimensionless input masses, m_l^{latt} and m_s^{latt} , are carefully chosen by subtracting the effect of the residual mass correction [13, 14]. The fifth-dimensional extent L_s is fixed to 12 for all ensembles. We have two different lattice spacings with two different lattice volumes for $145 \text{ MeV} \leq T \leq 250 \text{ MeV}$: $36^3 \times 12$ (p2 series) and $48^3 \times 12$ (p3) for the temporal lattice size $N_t = 12$, $48^3 \times 16$ (q2) and $64^3 \times 16$ (q3) for $N_t = 16$. Some of these parameters cover 130 MeV in the low temperature side, and 300 MeV in the high temperature side. For temperature $T \geq 250$ MeV, we also have $N_t = 10$ ensembles with lattice size $40^3 \times 10$ up to $T = 500$ MeV.

Both configuration generations and measurements were performed on Supercomputer Fugaku. We used Grid [15, 16] for configuration generation. The chiral condensate and susceptibility were measured with Grid/Hadrons [17], and the measurement of topological charge was performed using Bridge++ [18].

3. Chiral Condensate and Susceptibility

The chiral condensate serves as the order parameter for chiral symmetry breaking in QCD. At finite quark mass, it suffers from both additive and multiplicative divergences. To ensure it is well defined in the continuum limit, appropriate renormalization is required. The additive divergence behaves as $C^D(m + xm_{\text{res}})/a^2$, where the contribution xm_{res}/a^2 arises from the finite size of the domain wall fermion, which induces a similar effect as the mass term does. Here, $x = O(1)$ is a coefficient whose determination, along with that of C^D is from our 3-flavor MDWF study and detailed in [19]. The multiplicative divergence is removed by dividing the mass renormalization constant Z_m in the $\overline{\text{MS}}$ scheme, obtained from a next-to-next-to-leading order running [20].

The left panel of Fig. 1 presents the renormalized light quark chiral condensate at the physical quark mass as a function of temperature for two different volumes (with aspect ratios 3 and 4) on each of the $N_t = 12$ and $N_t = 16$ lattices. As expected, the chiral condensate decreases as temperature increases and eventually approaches zero at high temperatures where the chiral symmetry is restored. It is very challenging to locate the inflection point directly from the chiral condensate. For this purpose, we turn to the disconnected chiral susceptibility, χ_{disc} .

The disconnected chiral susceptibility quantifies the fluctuations of the chiral condensate. By definition, its construction as a variance ensures that the additive divergences cancel, leaving only a multiplicative divergence, which is removed by dividing by $(Z_m^{\overline{\text{MS}}})^2$. The right panel of Fig. 1 shows the renormalized disconnected chiral susceptibility as a function of temperature for $N_t = 12$ and $N_t = 16$, each with two different volumes. A pronounced peak, defining the pseudocritical temperature, is observed in the range of approximately 153-157 MeV. The chiral susceptibility does not exhibit significant volume or discretization effects, except in the q3 series. It should be noted that the statistics for the first three data points of the q3 series are around 300-400 configurations, substantially fewer than the approximately 2000 configurations for the other series. This explains the larger error bars for q3, particularly at the peak. Our estimate is more or less consistent with results obtained in the continuum limit using the HISQ and stout actions, which are 156.5(1.5) MeV [10] and 158.0(6) MeV [11], respectively. It is also consistent with other MDWF studies with $N_t = 8$ ensembles, which report 155(9) MeV [21] and $158.7_{-2.3}^{+2.6}$ MeV [7].

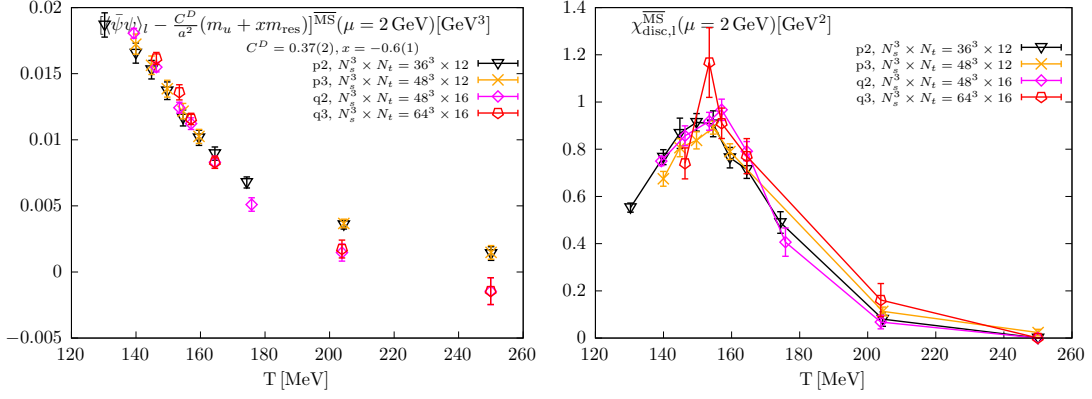


Figure 1: Chiral condensate of light quarks after multiplicative and additive renormalization (left) and chiral susceptibility after multiplicative renormalization.

4. Topological Susceptibility

We use a clover discretization of the topological charge after applying Wilson flow on the gauge field. The flow time is fixed to 5.0 in the lattice unit, which is intended not to introduce a new scale by hand in the physical unit. We have 9 Monte Carlo streams for each parameter set, and measure the topological charge every 10 trajectories after thermalization. Most of the data points have around 2000 measurements or more, except for the $64^3 \times 16$ lattice case. For this largest lattice volume, available configurations are still limited, and we use only about 300-400 configurations for $T \lesssim 160$ MeV.

In Figure 2, we plot typical examples of the flow time dependence of the topological charge squared. The vertical gray line indicates the flow time we adopt. Except for very high temperatures $T \geq 400$ cases, the value stays in the plateau region. Figure 3 shows the distributions of the topological charge Q for the same examples. The distributions at $T \geq 400$ are concentrated to $Q = 0$, where the value of Q is rounded into an integer. Especially, at $T = 500$ MeV, we observed only $Q = 0$ configurations. In evaluating the topological susceptibility $\chi_{\text{top}} = \langle Q^2 \rangle / V$, where V is the four-dimensional volume, we do not round Q into an integer.

The temperature dependence of the obtained topological susceptibility is plotted in Fig. 4. The finer lattice results systematically give smaller values than the coarser lattice. In the low temperature, the results with $N_t = 12$ overshoot the $T = 0$ result taken from [22], plotted as a gray band in the figure. This indicates that we have a sizable discretization effect at $N_t = 12$. In the low temperature phase, $T \leq 150$ MeV, we do not observe the volume dependence within the error. It is worth noting that our result at $N_t = 16$ is closer to the continuum limit in [3] with 2+1+1 flavor HISQ fermion than their $N_t = 16$ result. Their result at $T = 140$ MeV is $\chi_{\text{top}}^{1/4} \approx 72$ MeV in the continuum limit and 121 MeV with $N_t = 16$ calculated without rounding to an integer and eigenvalue reweighting, while our result with $N_t = 16$ is 78 MeV and 74 MeV at $T = 138, 145$ MeV, respectively.

At temperature $T = 250$ MeV, we have data from all three lattice spacings, $N_t = 10, 12,$ and 16 . Figure 5 suggests that a continuum extrapolation with linear in a^2 should be reasonable. The plot also implies that even at $N_t = 12$, there is a sizable finite- a effect. We reserve the systematic analysis of the continuum limit for future work. Another observation from this plot is that the finite

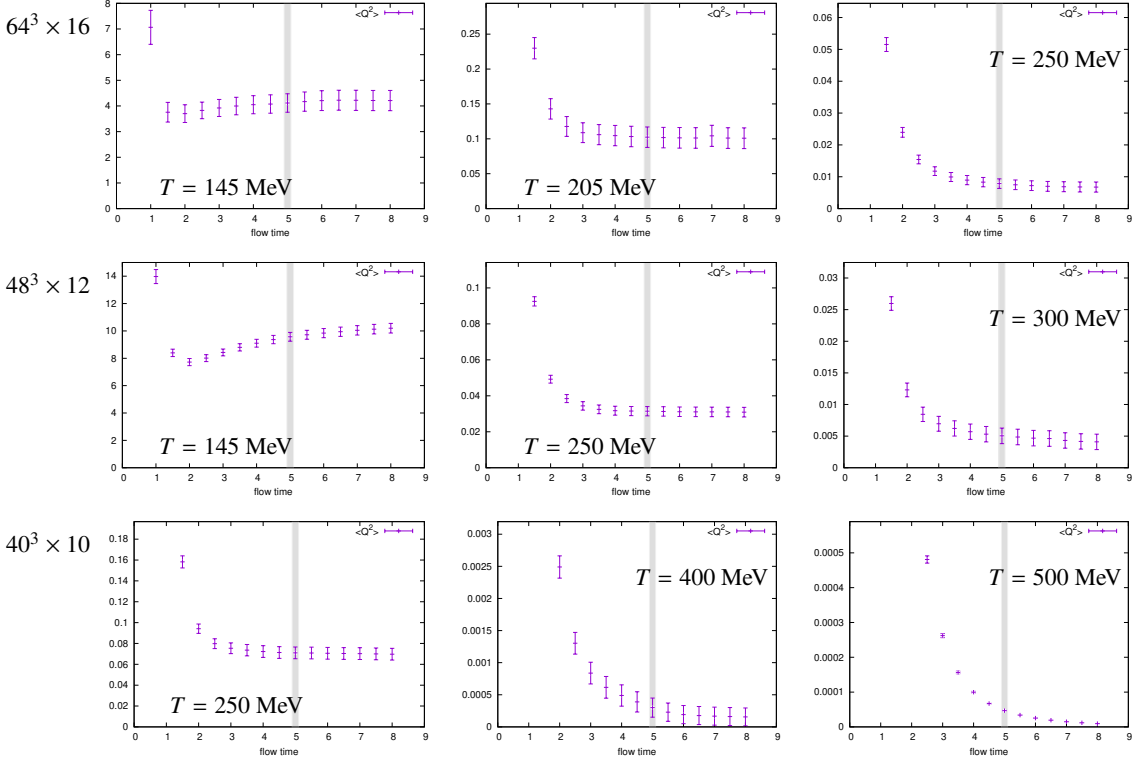


Figure 2: Flow time dependence of the topological charge squared.

volume effect can be relevant. The results with the aspect ratio 3 (triangle symbols) are smaller than those with the aspect ratio 4 (square symbols), although the size of the errors does not exclude the possibility of statistical fluctuation.

5. Summary and Outlook

We presented chiral condensate and disconnected susceptibility at finite temperature with physical point Möbius domain wall fermion with $N_t = 12$ and 16. The preliminary result of the pseudo-critical temperature is approximately 153-157 MeV. In the measurement of the topological susceptibility χ_{top} , we also combined $N_t = 10$ configurations at the high temperature end. Our result implies that the discretization error of χ_{top} with Möbius domain wall fermion seems smaller than other result with HISQ fermion, and the $N_t = 16$ result might be close to the continuum limit.

The simulation is still ongoing, and all the results presented here are preliminary. We will have more statistics, especially with the $64^3 \times 16$ lattice. The measurement of topological susceptibility at $T \geq 400$ MeV suffers from topology freezing, which requires analysis rather than simply measuring the global topological charge. Finally, we need careful comparisons with the results from different lattice fermions.

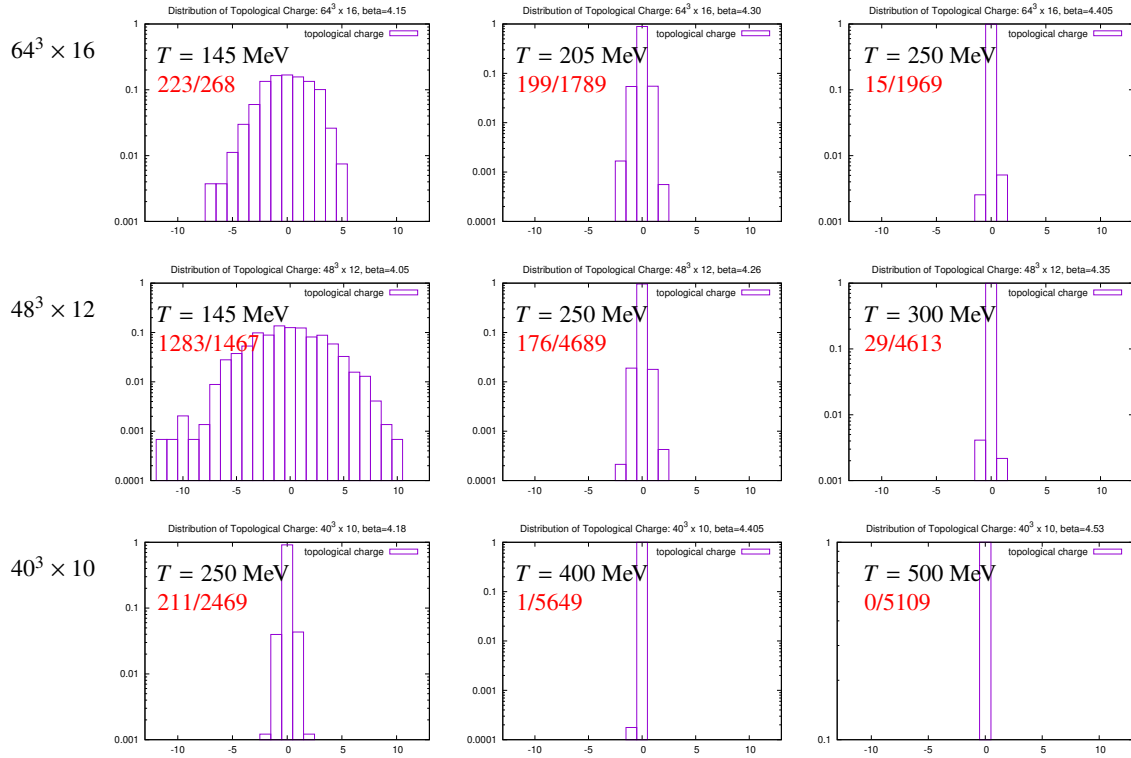


Figure 3: Distribution of the topological charge. The numbers denoted in red in each panel refer to the number of configurations with non-zero charges after rounding to an integer, and the measured configurations.

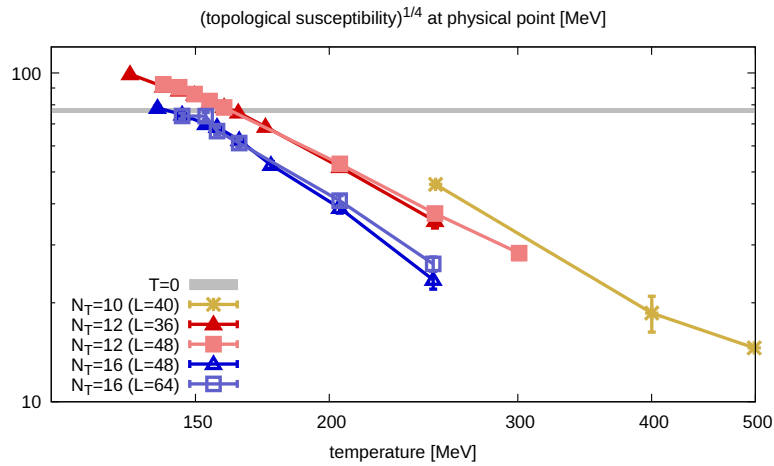


Figure 4: Temperature dependence of the 4th root of topological susceptibility. From coarse lattice to fine lattice: yellow ($N_t = 10$), red ($N_t = 12$), and blue ($N_t = 16$). The $T = 0$ value is taken from [22].

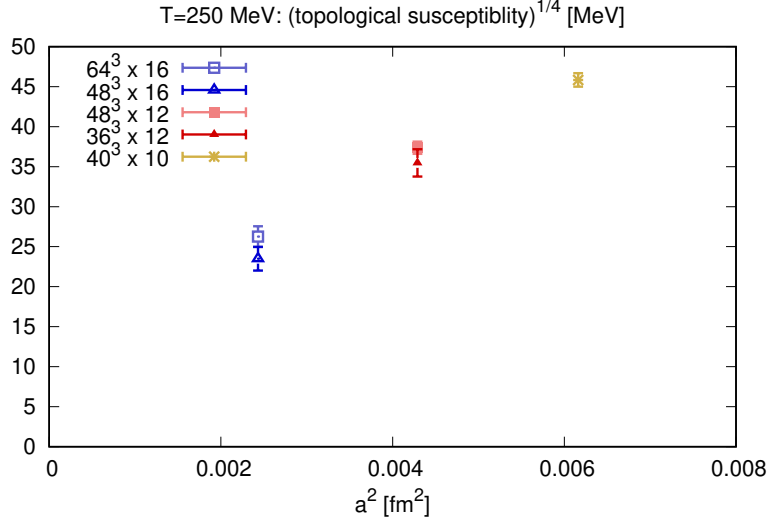


Figure 5: The lattice spacing dependence of the topological susceptibility at $T = 250$ MeV.

Acknowledgments

The project is supported by the MEXT as “Simulation for basic science: approaching the quantum era” (JPMXP1020230411) and Joint Institute for Computational Fundamental Science (JICFuS). We used Supercomputer Fugaku at RIKEN Center for Computational Science (R-CCS) for numerical simulation (HPCI project hp230207, hp240295, hp250224 and Usability Research ra000001). Y. Zhang and J. Goswami acknowledge support from the Deutsche Forschungsgemeinschaft (DFG) through the CRC-TR 211 “Strong-interaction matter under extreme conditions” (Project No. 315477589 - TRR 211).

References

- [1] C. Bonati, M. D’Elia, M. Mariti, G. Martinelli, M. Mesiti, F. Negro et al., *Axion phenomenology and θ -dependence from $N_f = 2 + 1$ lattice QCD*, *JHEP* **03** (2016) 155 [[1512.06746](#)].
- [2] P. Petreczky, H.-P. Schadler and S. Sharma, *The topological susceptibility in finite temperature QCD and axion cosmology*, *Phys. Lett. B* **762** (2016) 498 [[1606.03145](#)].
- [3] S. Borsanyi et al., *Calculation of the axion mass based on high-temperature lattice quantum chromodynamics*, *Nature* **539** (2016) 69 [[1606.07494](#)].
- [4] TWQCD collaboration, *Topological susceptibility in finite temperature QCD with physical ($u/d,s,c$) domain-wall quarks*, *Phys. Rev. D* **106** (2022) 074501 [[2204.01556](#)].
- [5] A.Y. Kotov, M.P. Lombardo and A. Trunin, *Topological observables and θ dependence in high temperature QCD from lattice simulations*, *JHEP* **09** (2025) 045 [[2502.15407](#)].

- [6] A. Athenodorou, C. Bonanno, C. Bonati, G. Clemente, F. D'Angelo, M. D'Elia et al., *Topological susceptibility of $N_f = 2 + 1$ QCD from staggered fermions spectral projectors at high temperatures*, *JHEP* **10** (2022) 197 [2208.08921].
- [7] R.V. Gavai, M.E. Jaensch, O. Kaczmarek, F. Karsch, M. Sarkar, R. Shanker et al., *Aspects of the chiral crossover transition in (2+1)-flavor QCD with Möbius domain-wall fermions*, *Phys. Rev. D* **111** (2025) 034507 [2411.10217].
- [8] Z. Fodor, A. Kotov, T.G. Kovacs and K.K. Szabo, *QCD thermodynamics with dynamical chiral fermions*, *PoS QCHSC24* (2025) 057 [2503.22243].
- [9] A.Y. Kotov et al. contribution to this volume.
- [10] HotQCD collaboration, *Chiral crossover in QCD at zero and non-zero chemical potentials*, *Phys. Lett. B* **795** (2019) 15 [1812.08235].
- [11] S. Borsanyi, Z. Fodor, J.N. Guenther, R. Kara, S.D. Katz, P. Parotto et al., *QCD Crossover at Finite Chemical Potential from Lattice Simulations*, *Phys. Rev. Lett.* **125** (2020) 052001 [2002.02821].
- [12] JLQCD collaboration, *Form factors of $B \rightarrow \pi \ell \nu$ and a determination of $|V_{ub}|$ with Möbius domain-wall fermions*, *Phys. Rev. D* **106** (2022) 054502 [2203.04938].
- [13] Y. Aoki, S. Aoki, H. Fukaya, S. Hashimoto, I. Kanamori, T. Kaneko et al., *2+1 flavor fine lattice simulation at finite temperature with domain-wall fermions*, *PoS LATTICE2021* (2022) 609 [2112.11771].
- [14] JLQCD collaboration, *Quark number susceptibility and conserved charge fluctuation for (2+1)-flavor QCD with Möbius domain wall fermions*, *PoS LATTICE2024* (2025) 168 [2501.03509].
- [15] P. Boyle, G. Cossu, A. Yamaguchi and A. Portelli, *Grid: A next generation data parallel C++ QCD library*, *PoS LATTICE2015* (2016) 023 [1512.03487].
- [16] N. Meyer, P. Georg, S. Solbrig and T. Wettig, *Grid on QPACE 4*, *PoS LATTICE2021* (2022) 068 [2112.01852].
- [17] A. Portelli, N. Asmussen, P. Boyle, F. Erben, V. Gülpers, R. Hodgson et al., *aportelli/hadrons: Hadrons v1.2*, Nov., 2020. 10.5281/zenodo.4293902.
- [18] S. Ueda, S. Aoki, T. Aoyama, K. Kanaya, H. Matsufuru, S. Motoki et al., *Development of an object oriented lattice QCD code 'Bridge++'*, *J. Phys. Conf. Ser.* **523** (2014) 012046.
- [19] Y. Zhang, Y. Aoki, S. Hashimoto, I. Kanamori, T. Kaneko and Y. Nakamura, *Three flavor QCD phase transition with Möbius domain wall fermions*, *PoS LATTICE2024* (2025) 193 [2501.15494].

- [20] K.G. Chetyrkin and A. Retey, *Renormalization and running of quark mass and field in the regularization invariant and \overline{MS} schemes at three loops and four loops*, *Nucl. Phys. B* **583** (2000) 3 [[hep-ph/9910332](#)].
- [21] T. Bhattacharya et al., *QCD Phase Transition with Chiral Quarks and Physical Quark Masses*, *Phys. Rev. Lett.* **113** (2014) 082001 [[1402.5175](#)].
- [22] JLQCD collaboration, *Topological susceptibility of QCD with dynamical Möbius domain-wall fermions*, *PTEP* **2018** (2018) 043B07 [[1705.10906](#)].